Canadian Journal of Physiology and Pharmacology
Revue canadienne de physiologie et pharmacologie

Cytosolic calcium changes affect the incidence of early afterdepolarizations in canine ventricular myocytes

Journal:	*Canadian Journal of Physiology and Pharmacology*
Manuscript ID:	cjpp-2014-0511
Manuscript Type:	Article
Date Submitted by the Author:	09-Dec-2014
Complete List of Authors:	Horvath, Balazs; University of Debrecen, Department of Physiology Hegyi, Bence; University of Debrecen, Department of Physiology Kistamas, Kornel; University of Debrecen, Department of Physiology Vaczi, Krisztina; University of Debrecen, Department of Physiology Banyasz, Tamas; University of Debrecen, Department of Physiology Magyar, Janos; University of Debrecen, Department of Physiology Szentandrassy, Norbert; University of Debrecen, Department of Physiology Nanasi, Peter; University of Debrecen, Department of Physiology
Keyword:	early afterdepolarizations, action potential duration, intracellular calcium concentration, cardiac myocytes, arrhythmogenesis

Cytosolic calcium changes affect the incidence of early afterdepolarizations in canine ventricular myocytes

Balázs Horváth[1,2,*], Bence Hegyi[1,*], Kornél Kistamás[1], Krisztina Váczi[1], Tamás Bányász[1], János Magyar[1,3], Norbert Szentandrássy[1,4], Péter P. Nánási[1,4]

[1]Department of Physiology, Faculty of Medicine, University of Debrecen, Hungary

[2]Faculty of Pharmacy, University of Debrecen, Debrecen, Hungary

[3]Division of Sport Physiology, Department of Physiology, Faculty of Medicine, University of Debrecen, Debrecen, Hungary

[4]Department of Dental Physiology and Pharmacology, Faculty of Dentistry, University of Debrecen, Hungary

[*]These authors have equally contributed to the study.

Correspondence: Péter P. Nánási, M.D., Ph.D., D.Sc.
Department of Physiology, University of Debrecen,
H-4012 Debrecen, Nagyerdei krt 98., Hungary.
Phone/Fax: +36-52-255575 / +36-52-255116
E-mail: nanasi.peter@med.unideb.hu

Abstract: The present study was designed to investigate the influence of cytosolic Ca^{2+} concentration ($[Ca^{2+}]_i$) on action potential duration (APD) and on the incidence of early afterdepolarizations (EADs) in canine ventricular cardiomyocytes. Action potentials (AP) of isolated cells were recorded using conventional sharp microelectrodes and concomitant $[Ca^{2+}]_i$ was monitored by the fluorescent dye, Fura-2. EADs were evoked at 0.2 Hz pacing rate by inhibiting the rapid delayed rectifier K^+ current with dofetilide, by activating the late sodium current with veratridine, or by activating the L-type calcium current with BAY K8644. These interventions progressively prolonged the AP and resulted in initiation of EADs. Reducing $[Ca^{2+}]_i$ by application of the cell-permeant Ca^{2+} chelator BAPTA-AM lengthened the AP at 1 Hz if it was applied alone or in the presence of veratridine and BAY K8644. BAPTA-AM, however, shortened the AP after pretreating the cells with dofetilide. The incidence of the evoked EADs was decreased by BAPTA-AM strongly in dofetilide and moderately in veratridine, while it was increased by BAPTA-AM in the presence of BAY K8644. Based on these experimental data changes in $[Ca^{2+}]_i$ have marked effects on APD as well as on EAD incidence, however, the underlying mechanisms may be different depending on the mechanism of EAD generation. As a consequence, reduction of $[Ca^{2+}]_i$ may eliminate EADs under some – but not all – experimental conditions.

Key words: early afterdepolarizations, action potential duration, intracellular Ca^{2+} concentration, arrhythmogenesis, canine myocytes, electrophysiology, fluorescent Ca^{2+} indicator dyes, Ca^{2+} chelators.

Introduction

Afterdepolarizations are defined as irregular membrane potential changes that disrupt the repolarization of the cardiac action potential. Early afterdepolarizations (EADs) appear during the plateau phase of an action potential with retarded terminal repolarization, while delayed afterdepolarizations (DADs) arise from the resting potential following complete repolarization (Hoffmann and Rosen 1981). Both types of afterdepolarizations may trigger extra action potentials in the neighboring cell, therefore they are considered as sources of cardiac arrhythmias including fatal ventricular fibrillation (Antzelevitch and Sicouri 1994). While DADs are known to be elicited by spontaneous Ca^{2+} release from the Ca^{2+}-overloaded sarcoplasmic reticulum (SR) leading to activation of Ca^{2+}-dependent inward currents, the mechanism of generation of EADs is still controversial (Fozzard 1992). Since EADs are typically evoked by interventions shifting the net membrane current towards inward direction during the action potential plateau and appear usually at slow pacing frequencies, EADs were explained by reactivation of a potentially regenerative inward current system (Hoffmann and Rosen 1981, Marban et al. 1986, January et al. 1988, January and Riddle 1989, Fozzard 1992), e.g. reopening of L-type Ca^{2+} channels (Zeng and Rudy 1995, Viswanathan and Rudy 1999, Bányász et al. 2003). On the other hand, experimental results have revealed the occurrence of apparently spontaneous Ca^{2+} release events during some types of EADs, which might be considered as a trigger based on their peculiar timing, i.e. the rise in $[Ca^{2+}]_i$ preceded depolarization similarly to observations made with DADs (Volders et al. 1997, Volders et al. 2000, Katra and Laurita 2005, Horvath et al. 2013). In the present study, therefore, the role of $[Ca^{2+}]_i$ changes in EAD generation was studied using three different EAD models. Dofetilide (inhibitor of the rapid delayer rectifier K^+ current, I_{Kr}), veratridine (activator of late Na^+ current, $I_{Na\text{-}Late}$) and BAY K8644 (activator of L-type Ca^{2+} current, I_{Ca}) are equally suitable to evoke EADs, since all of them may increase APD in the required extent. In addition, they cause a comparable elevation of $[Ca^{2+}]_i$. On the other hand, BAY K8644 directly modulates the opening/reopening of Ca^{2+} channels, which is not the case with veratridine and dofetilide. After elaborating the optimal experimental design, $[Ca^{2+}]_i$ was buffered following the development of EADs in each of the above models. This approach allowed to separate the

contribution of APD changes and $[Ca^{2+}]_i$ changes to generation of EADs. Isolated canine ventricular myocytes were chosen to be studied because the electrical properties (action potential morphology as well as the density and kinetics of the underlying ion currents) of these cells most resemble those of human myocardium (Szentandrássy et al. 2005, Szabó et al. 2005).

Materials and methods

Isolation of single canine ventricular myocytes

Adult mongrel dogs of either sex were anaesthetized with intramuscular injections of 10 mg/kg ketamine hydrochloride (Calypsol, Richter Gedeon, Hungary) + 1 mg/kg xylazine hydrochloride (Sedaxylan, Eurovet Animal Health BV, The Netherlands) according to protocols approved by the local ethical committee (license N^o: 18/2012/DEMÁB) in line with the ethical standards laid down in the Declaration of Helsinki in 1964 and its later amendments. Single myocytes were obtained by enzymatic dispersion using the segment perfusion technique, as described previously (Magyar et al. 2000). Briefly, the heart was quickly removed and washed in cold Tyrode solution. A wedge-shaped section of the ventricular wall supplied by the left anterior descending coronary artery was dissected, cannulated and perfused with a nominally Ca^{2+}-free Joklik solution (Minimum Essential Medium Eagle, Joklik Modification, Sigma-Aldrich Co. St. Louis, MO, USA) for 5 min. This was followed by 30 min perfusion with Joklik solution supplemented with 1 mg/ml collagenase (Type II, Worthington Biochemical Co., Lakewood, NJ, USA) and 0.2 % bovine serum albumin (Fraction V., Sigma) containing 50 μM Ca^{2+}. After gradually restoring the normal external Ca^{2+} concentration, the cells were stored in Minimum Essential Medium Eagle until use.

Experiments on isolated cells

All experiments were performed at 37 °C, maintained by an electronic temperature controller (Cell MicroControls, Norfolk, VA, USA). The rod-shaped viable cells showing clear striation were sedimented in a plexiglass chamber of 1 ml volume allowing continuous superfusion (at a rate of 2 ml/min) with Tyrode solution gassed with 100 %

O_2. The Tyrode solution contained (in mM): NaCl, 144; KCl, 5.6; $CaCl_2$, 2.5; $MgCl_2$, 1.2; HEPES, 5; and glucose 10; at pH=7.4. Action potentials of the isolated cells were monitored continously and the concomitant $[Ca^{2+}]_i$ transients were recorded in (1) Tyrode solution, (2) in the presence of dofetilide, veratridine or BAY K8644, and finally, (3) following exposure to BAPTA-AM. Drugs were obtained from Sigma-Aldrich Co. (St. Louis, MO, USA) except for BAY K8644 (Biotrend Chemikalien GmbH, Cologne, Germany), and dofetilide (Egis Pharmaceuticals Ltd., Budapest, Hungary).

Electrophysiology

Transmembrane potentials were recorded using 3 M KCl filled sharp glass microelectrodes having tip resistance between 20 and 40 MΩ. These electrodes were connected to the input of Multiclamp 700A or 700B amplifiers (Molecular Devices, Sunnyvale, CA, USA). The cells were paced through the recording electrode at steady cycle length of either 1 s (when recording action potentials -see **Figs. 1-2**) or 5 s (when recording EADs and $[Ca^{2+}]_i$ transients simultaneously - see **Figs. 3-6**) using 1-2 ms wide rectangular current pulses having amplitudes of twice the diastolic threshold. Since the cytosol was not dialyzed, time dependent changes in action potential morphology were negligible for the period of our experimental protocol lasting typically not longer than 45 min. Action potentials were digitized (at 200 kHz using Digidata 1322A, 1440A and 1200 A/D card, purchased from Axon Instruments Inc., Foster City, CA, USA) and stored for later analysis.

Recording of cytosolic Ca^{2+} concentration

$[Ca^{2+}]_i$ transients were assessed together with the transmembrane potential changes using the ratiometric dye, Fura-2, as described previously (Szigeti et al. 2000). Myocytes were loaded with the membrane-permeant form of Fura-2 (3 μM Fura-2-AM) for 30 min at room temperature in the presence of Pluronic F-127, then the cells were stored at 15 °C before the measurements. Cells were placed in a superfusion chamber on the stage of an inverted microscope (Eclipse TE2000-U, Nikon, Japan), warmed to 37 °C and viewed using a 40x oil immersion objective (CFI S-Fluor 40x oil, Nikon, Japan).

Fura-2 was excited with 340 and 380 nm monochromatic light. A xenon arc lamp (Ushio Deutschland GmbH, Steinhöring, Germany) was used as light source. Excitatory wavelengths were altered by a dual-wavelength excitation monochromator and an on-line connected computer (DeltaScan, Photon Technology International, New Brunswick, NJ, USA). Fluorescence emission was monitored at 510 nm using a R1527P photomultiplier tube (Hamamatsu Photonics Deutschland GmbH., Herrsching am Ammersee, Germany) at an acquisition rate of 200 Hz. Changes in intracellular free Ca^{2+} levels were approximated by the ratio of the fluorescence intensity obtained at 340 and 380 nm excitation after correction for nonspecific background fluorescence and recorded using FeliX32 Software & BryteBox Interface (Photon Technology International, New Brunswick, NJ, USA). Ten consecutive calcium transients were analyzed under each condition.

Determination of beat-to-beat variability of APD

Beat-to-beat variability of action potential duration was determined at 0.2 Hz when EADs were typically displayed. The series of 30 consecutive action potentials were analyzed to estimate variability according to the following formula:

$$V = \Sigma \left(\left| APD_{n+1} \textit{ minus } APD_n \right| \right) / [n_{beats} * \sqrt{2}]$$

where V is variability of APD, APD_n and APD_{n+1} indicate the durations of the n^{th} and $n+1^{th}$ action potentials, respectively, measured at 90% level of repolarization and n_{beats} denotes the number of consecutive beats analyzed.

Determination of EAD frequency

EADs were defined as inflexion of membrane potential change during the course of repolarization exceeding 3 mV in amplitude. EAD frequency was defined as the percentage of APs where at least 1 EAD could be observed. EAD frequency was determined for each cell using 30 consecutive action potentials in Tyrode solution, after 10 min of superfusion with dofetilide, veratridine or BAY K8644, and finally, after 30 min of superfusion with 5 µM BAPTA-AM.

Statistics

Results are expressed as mean ± SEM values. Statistical significance of differences was evaluated using one-way ANOVA followed by Student's t-test. Changes in the absolute number of EADs before and after BAPTA-AM application were evaluated by Fisher's exact test. Differences were considered significant when p was less than 0.05.

Results

Effects of BAPTA-AM on action potential duration at 1 Hz

Since the central issue of the present work was to study the effects of $[Ca^{2+}]_i$ changes on EAD generation, the concentration-dependent effects of dofetilide, veratridine and BAY K8644 (agents used to evoke EADs at low stimulation frequencies) on APD was studied at the pacing frequency of 1 Hz. At this fast driving rate EAD generation was absent, allowing direct comparison of drug-effects on APD within a relatively wide concentration range. According to the results presented in **Fig.1**, APD was increased significantly by all the three agents in a concentration-dependent manner. Moreover, these effects were practically identical at the concentration of 100 nM: the APD lengthening effects of dofetilide, veratridine and BAY K8644 were 84±6 ms (n=30), 76±7 ms (n=19) and 87±6 ms (n=6), respectively. Higher concentrations of veratridine and dofetilide caused larger lengthening of APD, while the effect of BAY K8644 was saturated at 100 nM. Prolongation of APD was accompanied by a marked upward shift in the plateau potential in the case of BAY K8644 and in a less pronounced way in the case of veratridine.

All of the above mentioned treatments increase $[Ca^{2+}]_i$ by different means. BAY K8644 increases I_{Ca} leading to a directly increased Ca^{2+} entry into the cells. Dofetilide prolongs the AP indirectly letting more Ca^{2+} to enter into the cells during the longer open state of the L-type calcium channels. Veratridine increases $[Na^+]_i$ and causes a reduced calcium extrusion through the sodium-calcium exchanger. In order to study the effects of $[Ca^{2+}]_i$ changes on APD under the conditions above, $[Ca^{2+}]_i$ was reduced by a Ca^{2+} chelator. The cells were loaded with the cell-permeant acetoxy-methylesther form of the Ca^{2+} chelator BAPTA (BAPTA-AM) and the cells were allowed to release BAPTA intracellularly as a consequence of intracellular esterase activity. As demonstrated in **Fig. 2.A**, superfusion with 5 μM BAPTA-AM for 30 min progressively increased APD. The

configuration of action potentials was also characteristically altered: the plateau potential was markedly elevated by BAPTA-AM, a change congruent with larger amplitude of I_{Ca} due to diminished Ca^{2+}-dependent inactivation. APD was increased by BAPTA-AM alone as well as when BAPTA-AM was applied in the presence of veratridine or BAY K8644, but not after pretreatment with dofetilide (**Fig. 2.B-E**). Actually veratridine and BAY K8644 significantly enhanced the APD lengthening effect of BAPTA-AM, while a significant APD shortening was observed when the cells were exposed to BAPTA-AM in the presence of dofetilide (**Fig.2.F**).

Effects of BAPTA-AM on EAD incidence at 0.2 Hz

In each of the three EAD models studied drug-effects were combined with consequences of slow driving rate. Dofetilide strongly lengthened APs and increased the beat-to-beat variability of APD markedly, which was accompanied by development of EADs in all of the 10 cells exposed to 300 nM dofetilide for 10 min. In 6 of these cells EADs were present continuously, while in 4 cells the frequency of EAD varied between 20 % and 70 % of the total recording period. All these changes were reverted by superfusion of 5 μM BAPTA-AM for 30 min, although the reversion was not complete. EADs fully disappeared in 8 out of the 10 cells, and an EAD frequency of only 20-40 % was obtained in the remaining 2. The high average value of EAD frequency observed in dofetilide (77±10%) was decreased to 5±4 % in the presence of BAPTA-AM ($p<0.05$, $n=10$). APD variability was also reduced significantly by BAPTA-AM (**Fig. 3**).

In the presence of 300 nM veratridine EAD frequency was lower than observed with dofetilide. This could not been overcome even if the concentration of veratridine was elevated up to 1 μM (not shown). Although EADs developed in all of the 18 cells exposed to veratridine, the average frequency of EADs was only 37.4±6.4 %, which was reduced by BAPTA-AM superfusion to 22.4±6.0 % ($p<0.05$, $n=18$). Similarly to EAD frequency, the variability of APD was also moderately but significantly diminished by BAPTA-AM (**Fig. 4**).

EADs developed in 16 out of the 21 cells exposed to 200 nM BAY K8644, displaying an EAD frequency of 56.8±9.2 %. APD variability was also increased - similarly to results obtained with dofetilide or veratridine. In contrast to these results,

however, superfusion with BAPTA-AM further increased EAD-frequency to 70.4±8.2 % ($p<0.05$, n=21) since 19 cells displayed EADs following BAPTA-AM superfusion, while APD variability remained unaltered (**Fig. 5**).

Effects of BAPTA-AM on $[Ca^{2+}]_i$ transients at 0.2 Hz

Using the same protocol applied for EAD measurements, changes in cytosolic free Ca^{2+} concentration was recorded in the presence of 300 nM dofetilide, 300 nM veratridine and 200 nM BAY K8644 (**Fig. 6**). Diastolic and systolic $[Ca^{2+}]_i$ levels were significantly increased by all of these drugs, resulting in drastic increases in $[Ca^{2+}]_i$ transient amplitudes. These changes in the peak $[Ca^{2+}]_i$ values and $[Ca^{2+}]_i$ amplitudes were readily reverted by exposure to 5 μM BAPTA-AM for 30 min, furthermore, $[Ca^{2+}]_i$ amplitudes were significantly lower than their respective control values in the case of dofetilide and BAY K8644, but not in the case of veratridine. Diastolic $[Ca^{2+}]_i$, however, further increased during the time of BAPTA-AM superfusion.

Discussion

In the present study the effect of $[Ca^{2+}]_i$ changes on the incidence of EADs were studied using three models of EADs. EADs were evoked by I_{Kr} blockade (dofetilide), activation of $I_{Na\text{-}Late}$ (veratridine) and activation of I_{Ca} (BAY K8644). Each of these interventions resulted in initiation of EADs at 0.2 Hz pacing frequency. Superfusion of the myocytes with the Ca^{2+} chelator BAPTA-AM (in the continuous presence of the previously applied agent) decreased $[Ca^{2+}]_i$ drastically, while its effect on the EAD frequency was variable depending on the actual combination of APD and $[Ca^{2+}]_i$ changes. BAPTA-AM markedly reduced APD as well as EAD frequency in the presence of dofetilide, emphasizing the primary role of APD lengthening in the generation of EADs (January et al. 1991, January and Moscucci 1992). On the other hand, both APD and EAD frequency were increased by BAPTA-AM in the presence of BAY K8644 - in accordance with the concept above. However, if EAD incidence was dependent exclusively on APD, BAPTA-AM should have increased EAD frequency in veratridine due to the strong APD lengthening effect of BAPTA-AM in veratridine (as demonstrated in **Fig. 2.C** and **F**). Clearly, this was not the case, since chelation of $[Ca^{2+}]_i$ *decreased* EAD frequency (and also variability of APD)

after veratridine treatment. More explicitely, BAPTA-AM decreased EAD frequency in spite of its APD lengthening effect. This is an evidence indicating that elevation of $[Ca^{2+}]_i$ is really a considerable factor of EAD incidence, capable to generate both types of afterdepolarizations.

Another argument against the exclusive role of APD in EAD generation arises when the effects of BAPTA-AM in the presence of BAY K8644 and veratridine are compared. BAPTA-AM evoked comparable prolongations of APD in the presence of the two agents (**Fig. 2.F**), while its effect on EAD frequency was the opposite in BAY K8644 (enhancement) and veratridine (reduction). Taking into account that the effect of BAPTA-AM on $[Ca^{2+}]_i$ transients was similar in veratridine and BAY K8644 (in fact, the amplitude of $[Ca^{2+}]_i$ transient was even reduced below the control level by BAPTA-AM in BAY K8644)) the divergent effects on EAD frequency cannot be attributed to changes in $[Ca^{2+}]_i$. It is likely that the augmentation of I_{Ca} by BAY K8644 - resulting in a larger population of Ca^{2+} channels mediating more late Ca^{2+} current - is the substrate for the enlarged EAD frequency in BAY K8644, which was further aggravated by reduction of $[Ca^{2+}]_i$ probably due to shifting the Ca^{2+} channels towards a non-inactivated state.

In summary, changes in $[Ca^{2+}]_i$ may have marked effects on EAD incidence, however, the underlying mechanisms may be different depending on the mechanism of EAD generation. As a consequence, reduction of $[Ca^{2+}]_i$ may eliminate EADs under some - but not all - experimental conditions.

Acknowledgements

Financial support was provided by grants from the Hungarian Scientific Research Fund (OTKA-K100151, OTKA-K109736, OTKA-K101196, OTKA-PD101171 and OTKA-NK104331). Further support was obtained from the Hungarian Government and the European Community (TAMOP-4.2.2.A-11/1/KONV-2012-0045 research project) and National Excellence Program (TAMOP-4.2.4.A/2-11/1-2012-0001) to BH and Bolyai János Research Scholarship to NS. The authors thank Miss Éva Sági for excellent technical assistance. The authors declare that they have no conflict of interest.

References

Antzelevitch, C., Sicouri, S. 1994. Clinical relevance of cardiac arrhythmias generated by afterdepolarizations. J. Am. Coll. Cardiol. **23**: 259-277.

Bányász, T., Fülöp, L., Magyar, J., Szentandrássy, N., Varró, A., Nánási, P.P. 2003. Endocardial versus epicardial differences in L-type calcium current in canine ventricular myocytes studied by action potential voltage clamp. Cardiovasc. Res. **58**: 66-75.

Fozzard, H.A. 1992. Afterdepolarizations and triggered activity. Basic Res. Cardiol. **87**: Suppl. 2, 105-113.

Horvath B, Banyasz T, Jian Z, Hegyi B, Kistamas K, Nanasi PP, Izu LT, Chen-Izu Y. 2013. Dynamics of the late Na^+ current during cardiac action potential and its contribution to afterdepolarizations J. Mol. Cell. Cardiol. **64**: 59-68.

Hoffmann, B.F., Rosen, M.R. 1981. Cellular mechanisms for cardiac arrhythmias. Circ. Res. **49**: 1-15.

January, C.T., Riddle, J.M., Salata, J.J. 1988. A model for early afterdepolarizations: induction with the Ca^{2+} channel agonist Bay K 8644. Circ. Res. **62**: 563-571.

January, C.T., Riddle, J.M. 1989. Early afterdepolarizations: mechanism of induction and block. A role for L-type Ca^{2+} current. Circ. Res. **64**: 977-990.

January, C.T., Chau, V., Makielski, J.C. 1991. Triggered activity in the heart: cellular mechanisms of early after-depolarizations. Eur. Heart J. **12:** Suppl. F, 4-9.

January, C.T., Moscucci, A. 1992. Cellular mechanisms of afterdepolarizations. Ann. N.Y. Acad. Sci. **644:** 23-32.

Katra, R.P., Laurita, K.R. 2005. Cellular mechanism of calcium-mediated triggered activity in the heart. Circ. Res. **96**: 535-542.

Magyar, J., Iost, N., Körtvély, Á., Bányász, T., Virág, L., Szigligeti, P., Varró, A., Papp, J.Gy., Nánási, P.P. 2000. Effects of endothelin-1 on calcium and potassium currents in undiseased human ventricular myocytes. Pflügers Arch. **441**: 144-149.

Marban, E., Robinson, S.W., Wier, W.G. 1986. Mechanisms of of arrhythmogenic delayed early afterdepolarizations in ferret ventricular muscle. J. Clin. Invest. **78**: 1185-1192.

Szabó, G., Szentandrássy, N., Bíró, T., Tóth, I.B., Czifra, G., Magyar, J., Bányász, T., Varró, A., Kovács, L., Nánási, P.P. 2005. Asymmetrical distribution of ion channels in canine and human left-ventricular wall: epicardium versus midmyocardium. Pflügers Arch. **450**: 307-316.

Szentandrássy, N., Bányász, T., Bíró, T., Szabó, G., Tóth, B., Magyar, J., Lázár, J., Varró, A., Kovács, L., Nánási, P.P. 2005. Apico-basal inhomogeneity in distribution of ion channels in canine and human ventricular myocardium. Cardiovasc. Res. **65**: 851-860.

Szigeti, Gy., Bányász, T., Magyar, J., Körtvély, Á., Szigligeti, P., Kovács, L., Jednákovits, A., Nánási, P.P. 2000. Effects of bimoclomol, the novel heat shock protein coinducer, in dog ventricular myocardium. Life Sci. **67**: 73-79.

Volders, P.G.A., Kulcsár, A., Vos, M.A., Sipido, K.R., Wellens, H.J.J., Lazzara, R., Szabo, B. 1997. Similarities between early and delayed afterdepolarizations induced by isoproterenol in canine ventricular myocytes. Cardiovasc. Res. **34**: 348-359.

Volders, P.G.A., Vos, M.A., Szabo, B., Sipido, K.R., Marieke de Groot, S.H., Gorgels, A.P.M., Wellens, H.J.J., Lazzara, R. 2000. Progress in the understanding of cardiac early

afterdepolarizations and torsades de pointes: time to revise current concepts. Cardiovasc. Res. **46**: 376-392.

Viswanathan, P.C., Rudy, Y. 1999. Pause induced early afterdepolarizations in long QT syndrome: a simulation study. Cardiovasc. Res. **42:** 530-542.

Zeng, J., Rudy, Y. 1995. Early afterdepolarizations in cardiac myocytes: mechanism and rate dependence. Biophys. J. **68:** 949-964.

Figure legends

Fig.1. Concentration-dependent effects of dofetilide (**A, B**), veratridine (**C, D**), and BAY K8644 (**E, F**) on action potential configuration (**A, C, E**) and duration (**B, D, F**) at 1 Hz. Each drug concentration was applied for 5 min. Columns and bars are means ± SEM, asterisks denote significant changes from control, numbers in parentheses indicate the number of cells studied.

Fig.2. Time-dependent effects of 5 μM BAPTA-AM alone (n=18, **A, B**), in the presence of 100 nM veratridine (n=7, **C**), 100 nM BAY K8644 (n=6, **D**) and 100 nM dofetilide (n=7, **E**) at 1 Hz. Superfusion with BAPTA-AM started after 5 min period of drug-pretreatment. Open circles denote data without BAPTA-AM (with or without drug-pretreatment), filled circles represent APD values observed in the presence of BAPTA-AM. Average results obtained at the 15th and 25th min of superfusion with BAPTA-AM are presented in panel **F**. Symbols, columns and bars indicate means ± SEM, asterisks denote significant differences between pre-BAPTA-AM and post-BAPTA-AM values, + symbols in panel **F** indicate significant differences in actions of BAPTA-AM after drug-pretreatment *versus* BAPTA-AM alone.

Fig.3. Effect of BAPTA-AM on EAD incidence in the presence of dofetilide at 0.2 Hz. Representative records of membrane potential changes (**A, B, C**) and cytosolic Ca^{2+} signals (**D, E, F**) obtained in control (**A, D**), in the presence of 300 nM dofetilide for 10 min (**B, E**) and after superfusion with 5 μM BAPTA-AM in the presence of dofetilide for 30 min (**C, F**). **G, H**: Average results obtained on EAD frequency (**G**) and APD variability (**H**) in 10 myocytes. Each small open circle in panel **G** represents an individual cell showing its EAD frequency, filled squares indicate average values. Symbols, columns and bars indicate means ± SEM, asterisks denote significant differences from control, + symbols indicate BAPTA-AM induced significant changes.

Fig.4. Effect of BAPTA-AM on EAD incidence in the presence of veratridine at 0.2 Hz. Representative records of membrane potential changes (**A, B, C**) and cytosolic Ca^{2+} signals

(**D, E, F**) obtained in control (**A, D**), in the presence of 300 nM veratridine for 10 min (**B, E**) and after superfusion with 5 μM BAPTA-AM in the presence of veratridine for 30 min (**C, F**). **G, H**: Average results obtained on EAD frequency (**G**) and APD variability (**H**) in 18 myocytes. Each small open circle in panel **G** represents an individual cell showing its EAD frequency, filled squares indicate average values. Symbols, columns and bars indicate means ± SEM, asterisks denote significant differences from control, + symbols indicate BAPTA-AM induced significant changes.

Fig.5. Effect of BAPTA-AM on EAD incidence in the presence of BAY K8644 at 0.2 Hz. Representative records of membrane potential changes (**A, B, C**) and cytosolic Ca^{2+} signals (**D, E, F**) obtained in control (**A, D**), in the presence of 200 nM BAY K8644 for 10 min (**B, E**) and after superfusion with 5 μM BAPTA-AM in the presence of BAY K8644 for 30 min (**C, F**). **G, H**: Average results obtained on EAD frequency (**G**) and APD variability (**H**) in 21 myocytes. Each small open circle in panel **G** represents an individual cell showing its EAD frequency, filled squares indicate average values. Symbols, columns and bars indicate means ± SEM, asterisks denote significant differences from control, + symbols indicate BAPTA-AM induced significant changes.

Fig.6. Effect of BAPTA-AM on intracellular Ca^{2+} transients recorded in the presence of dofetilide (**A-C**), veratridine (**D-F**) and BAY K8644 (**G-I**) at 0.2 Hz. The experimental protocol was identical to that used in Figs. 3-5. Diastolic (**A, D, G**), systolic $[Ca^{2+}]_i$ (**B, E, H**), as well as the amplitude of the $[Ca^{2+}]_i$ transient (**C, F, I**) are expressed as fluorescent ratios (F_{340} / F_{380}). Columns and bars indicate means ± SEM, asterisks denote significant differences from control, + symbols indicate BAPTA-AM induced significant changes.

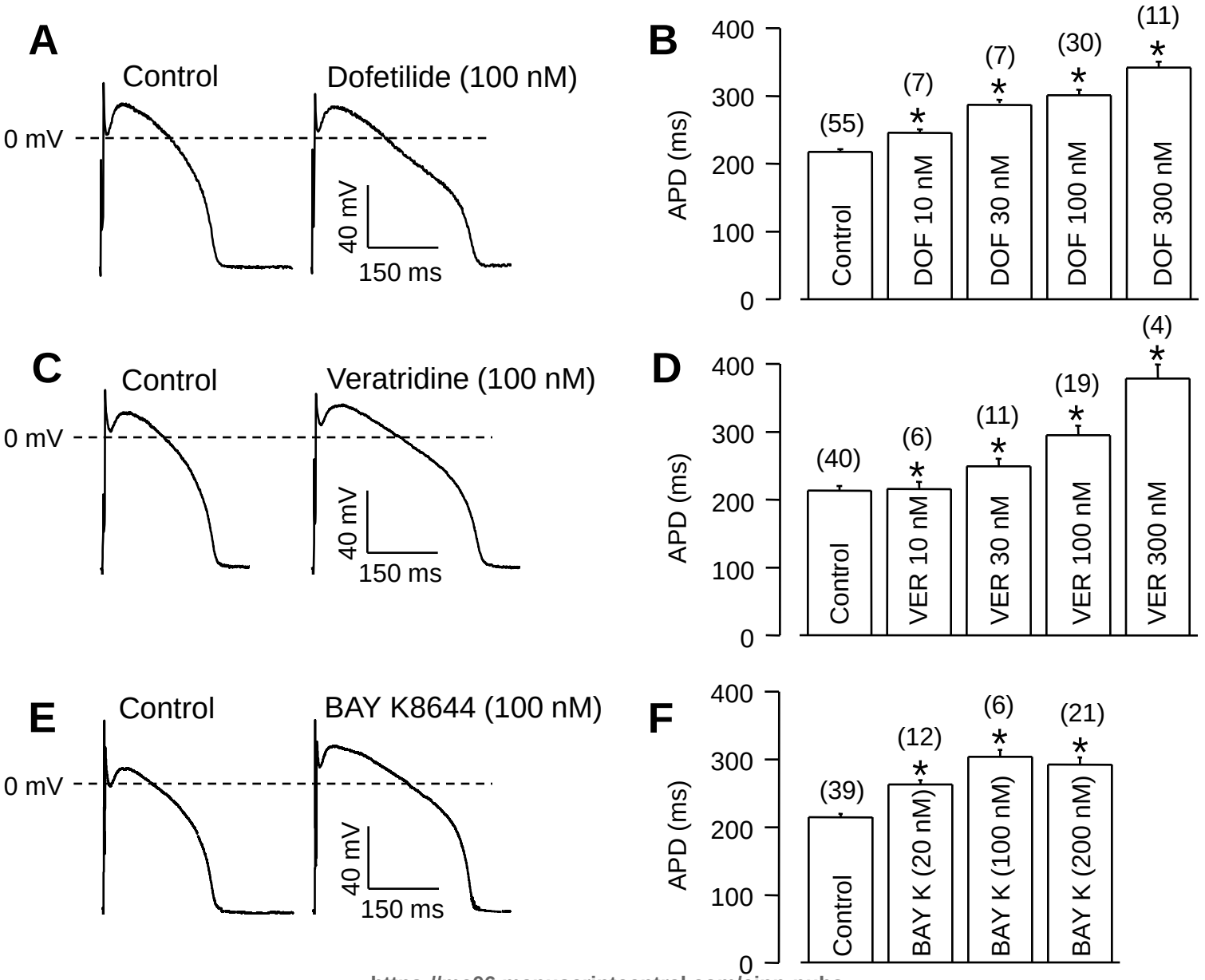
A
Control
Dofetilide (100 nM)
0 mV
40 mV
150 ms
B
APD (ms)
400
300
200
100
0
(55)
(7)
(7)
(30)
(11)
Control
DOF 10 nM
DOF 30 nM
DOF 100 nM
DOF 300 nM
C
Control
Veratridine (100 nM)
0 mV
40 mV
150 ms
D
APD (ms)
400
300
200
100
0
(40)
(6)
(11)
(19)
(4)
Control
VER 10 nM
VER 30 nM
VER 100 nM
VER 300 nM
E
Control
BAY K8644 (100 nM)
0 mV
40 mV
150 ms
F
APD (ms)
400
300
200
100
0
(39)
(12)
(6)
(21)
Control
BAY K (20 nM)
BAY K (100 nM)
BAY K (200 nM)

Fig. 1

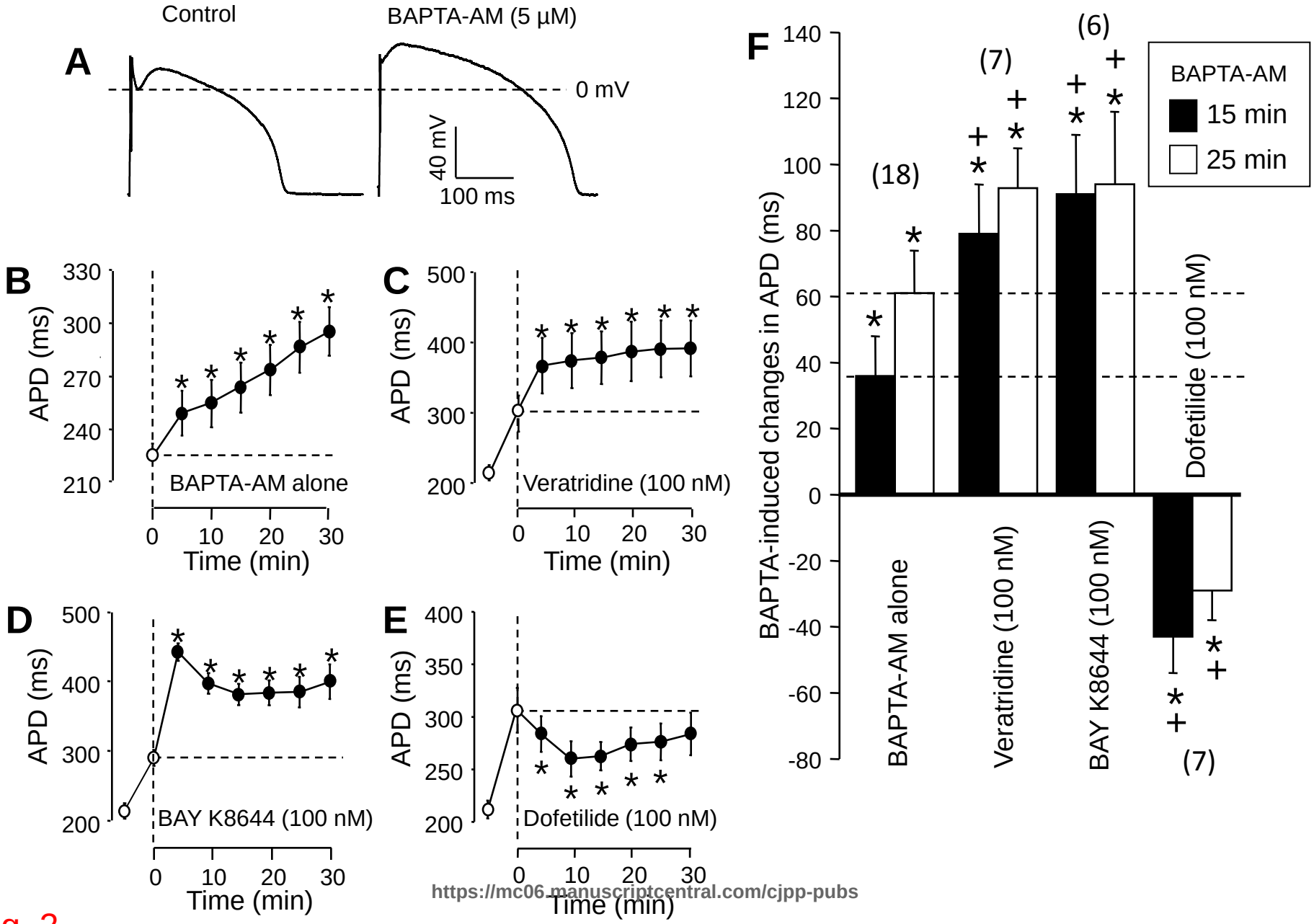

Fig. 2

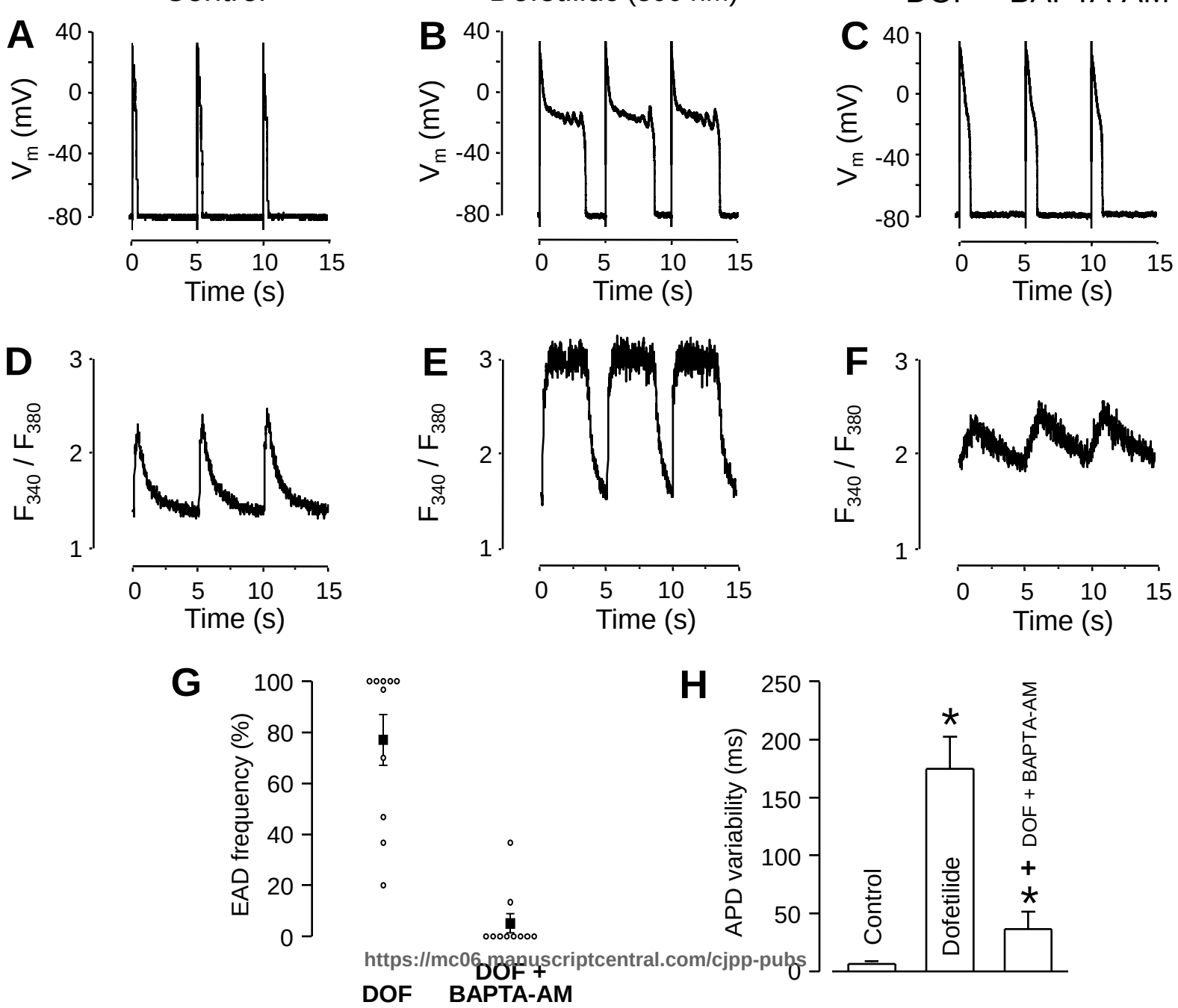

Fig. 3

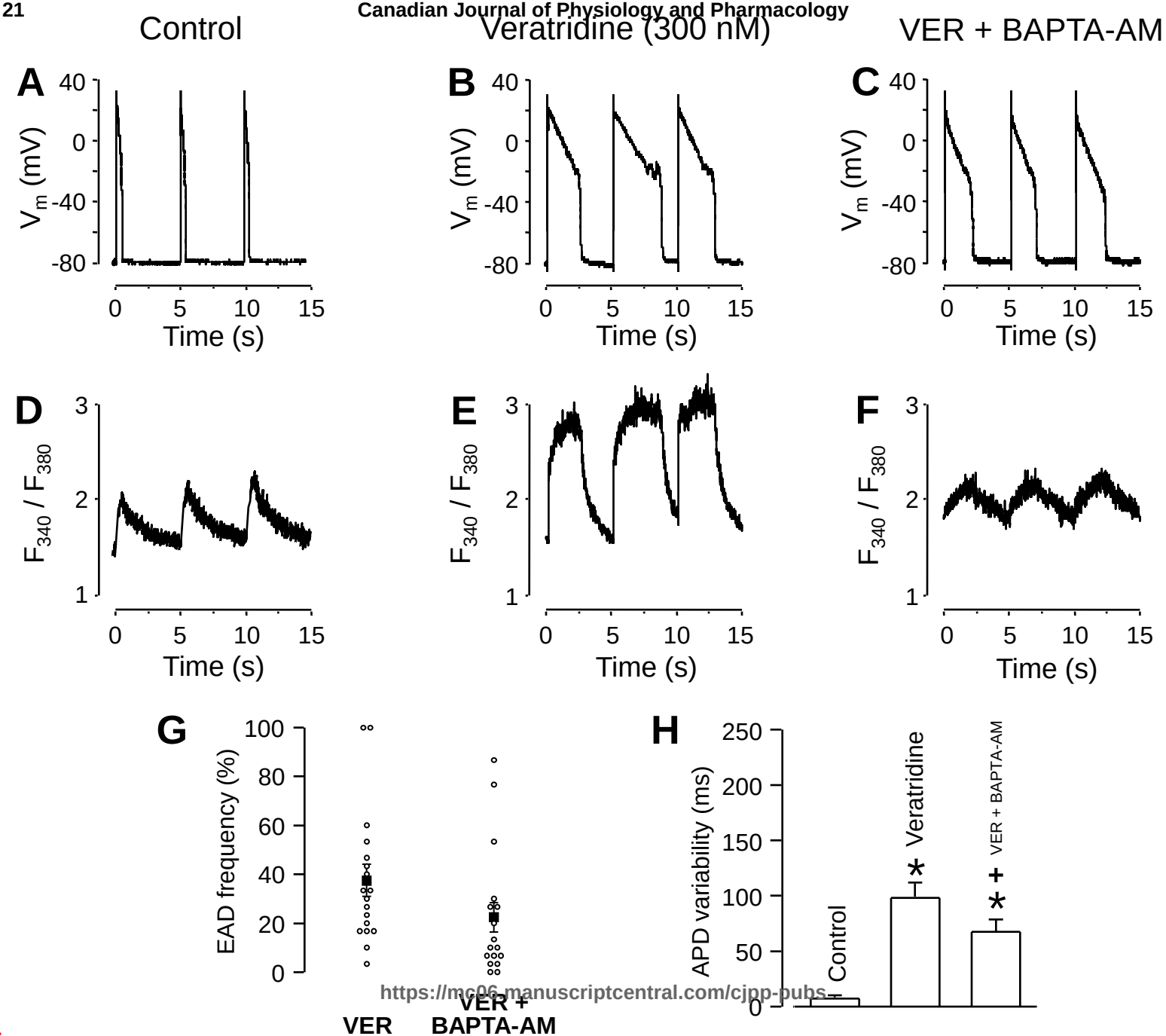

Fig. 4

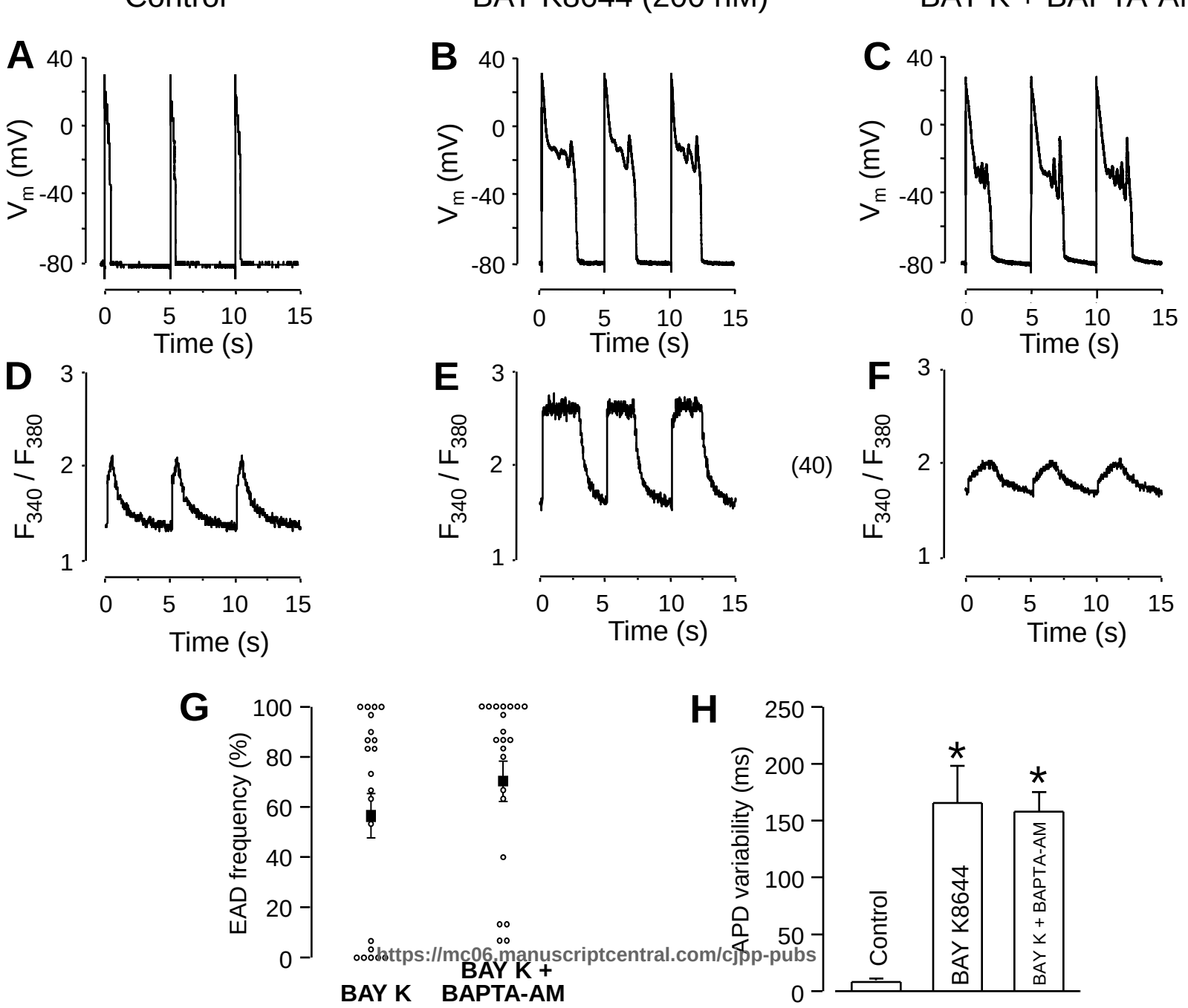

Fig. 5

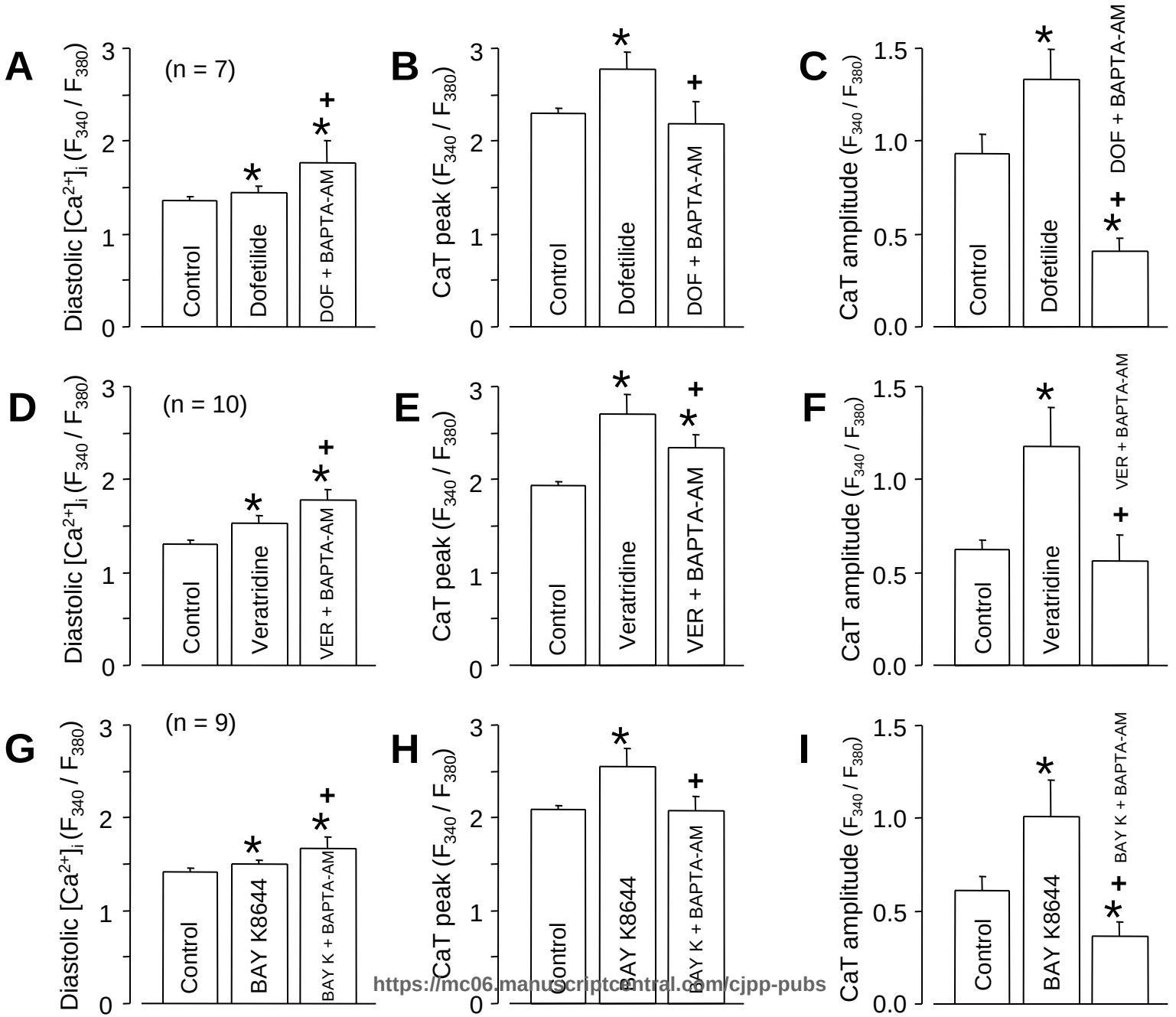

Fig. 6